

Vacuum Energy of Non–Supersymmetric \tilde{S} Heterotic String Models

Luke A. Detraux^{1*},

Alonzo R. Diaz Avalos^{1†}, Alon E. Faraggi^{1‡} and Benjamin Percival^{1,2§}

¹ *Dept. of Mathematical Sciences, University of Liverpool, Liverpool L69 7ZL, UK*

² *Dept. of Natural Sciences, Manchester Metropolitan University, M15 6BH, UK*

Abstract

We use the free fermionic formulation of the heterotic–string in four dimensions to study the vacuum structure and energy of non–supersymmetric tachyon free models that correspond to compactifications of tachyonic vacua of the ten dimensional heterotic–string. We explore the class of heterotic $SO(10)$ non–supersymmetric models constructed from the \tilde{S} –model in the Free Fermionic Formalism, and investigate the dependence of the potential on the geometric moduli. This paper will explore a sample of 10^9 string vacua to find the frequency of viable models, classifying these vacua by the following fertility criteria: tachyon presence; number of spinorial $\mathbf{16}/\overline{\mathbf{16}}$ representations; vectorial $\mathbf{10}$ states; Top Quark Mass Coupling compatibility. Of these we find those that mimic supersymmetric models with equal number of bosons and fermions at the massless level - $a_{00} = 0$. Tachyon free models occur with a frequency of 5.309×10^{-3} . Furthermore, models that fulfil the rest of the phenomenological fertility conditions and the additional condition on a_{00} occur with probability 4.0×10^{-9} . We analyse the partition functions and study the moduli dependence of such models, finding that almost all fertile models have finite, positive potential at the Free Fermionic Point, with 2 out of 84 of the fertile cores having negative, finite potential. We demonstrate that the Free Fermionic Point is not necessarily a minimum in the potential. This work provides further evidence that supersymmetry may not be a necessary ingredient of phenomenological models, recreating many of the desirable features of such models without employing supersymmetry.

*E-mail address: ldetraux@liverpool.ac.uk

†E-mail address: a.diaz-avalos@liverpool.ac.uk

‡E-mail address: alon.faraggi@liverpool.ac.uk

§E-mail address: b.percival@mmu.ac.uk

Contents

1	Introduction	1
2	The \tilde{S}-Models	3
3	Analysis of Tachyonic Sectors	4
4	Analysis of Massless Sectors	6
4.1	Spinorials	6
4.2	Vectorials	8
4.3	Hidden Sectors	8
4.4	Other Massless States	9
4.5	Top Quark Mass Coupling	9
4.6	Enhancements	10
4.7	$N_b - N_f = 0$ at the Massless Level	11
5	Partition Function and Potential	12
5.1	Partition Function	12
5.2	Potential	14
6	Classification Results	15
7	Example Model	16
8	Discussion and Conclusion	20

1 Introduction

The Standard Model (SM) of particle physics provides viable parameterisation of all observable data to date concerning particles and their interactions via three of the four fundamental forces, and it may remain viable up to the Grand Unified Theory scale, or the Planck scale, where the gravitational effects are non-negligible. However the SM is incomplete, and one of the outstanding problems in this construction is the Cosmological Constant Problem. String theory acts as a unique laboratory to explore the synthesis of the gauge and gravitational interactions within a self-consistent framework, and probe the open questions in the SM. Phenomenological string models are constructed that reproduce the main phenomenological characteristics of the Minimal Supersymmetry Standard Model (MSSM) [1, 2, 3]. The early constructions since the late 1980s generally possessed $N = 1$ spacetime supersymmetry that guarantees the stability of the vacuum and simplifies the analysis in some respect by guaranteeing a vanishing Cosmological Constant at one-loop.

More recently non-supersymmetric string vacua have been of interest as well [4, 5, 6, 7, 8, 9], and the stability of their potential have been investigated infrequently [10, 11, 12, 13]. These studies mainly focus on compactifications of the $SO(16) \times SO(16)$ heterotic-string, which is tachyon free in ten dimensions [14, 15, 16, 17, 18]. In general, however, compactifications of the $SO(16) \times SO(16)$ heterotic-string to four dimensions give rise to physical tachyonic states in the spectrum of the four dimensional models, which are

projected from the spectrum by Generalised Gliozzi–Scherk–Olive (GGSO) projections. In addition, heterotic string theory gives rise to non-supersymmetric vacua that are tachyonic in ten dimensions [14, 15]. Physical tachyons can then be projected from the spectrum in the compactified theory by GGSO projections [19, 20] as in the $SO(16) \times SO(16)$ case, and so it is prudent to study the phenomenological properties and stability of these vacua as well. Over the past few years several studies along these lines has been pursued [19, 20, 21, 22, 23], as well as studies of non-supersymmetric four dimensional models that correspond to compactifications of the $SO(16) \times SO(16)$ heterotic-string [4, 5, 10, 24, 25, 26, 27]. A specific class of these studies are on internal spaces that correspond to $\mathbb{Z}_2 \times \mathbb{Z}_2$ orbifolds of six dimensional toroidal lattices, and are analysed by using the Free Fermionic Formulation (FFF) [28, 29] of the heterotic-string in four dimensions. Within these models, those that descend from the $SO(16) \times SO(16)$ heterotic-string are dubbed as S -models, whereas those that descend from a specific tachyonic ten dimensional vacuum are dubbed as \tilde{S} -models. We refer the readers to the literature for more detailed explanation of this nomenclature [19, 20]. To date the value of the cosmological constant and its dependence on the structure of the vacuum has been exclusively studied in the context of S -models[¶]. We extend the analysis to \tilde{S} -models.

In this paper we will build a non-supersymmetric $SO(10)$ models with the $\tilde{\mathbf{S}}$ vector as one of 12 basis vectors based on the $\overline{\text{NAHE}}$ set using the Free Fermionic Formalism. Details of the construction are given in Section 2. From the possible 2^{66} independent GGSO phase matrices, our program, written in C++, takes a random sample of 10^9 matrices and classifies these models by the fertility conditions developed in [21]. These fertility conditions are: level-matched tachyon projection; compatibility with the three generations of the SM fermions; compatibility with the Higgs doublet; maintaining Top Quark Mass Coupling (TQMC). With comparison to supersymmetric models in mind, we also identify models with massless fermion and boson cancellation, $a_{00} = N_B - N_F = 0$. Section 3 details the origins of the problematic tachyonic sectors and their survival conditions, followed by analysis of the massless spectrum in Section 4.

In the second half of this paper we move away from the Free Fermionic Point, (FFP), referred to as the fermionic point or fermionic radius in [30], to analyse the partition function and resultant potential of these fertile cores. This is achieved by bosonising the internal worldsheet fermions, through the relationship $\partial X^I \approx \sqrt{\alpha'} y^I \omega^I$, where the fermionic radius $R = \sqrt{\frac{\alpha'}{2}}$. We demonstrate that stability of a model is not exclusive to S -models and many of the features of supersymmetric and non-supersymmetric S -models can be replicated in non-supersymmetric \tilde{S} -models. In particular, we demonstrate that stable minima in the potential can be found for non-supersymmetric \tilde{S} -models at or close to the FFP, when the geometric moduli, $T^{(1)}$ and $U^{(1)}$ are varied in imaginary direction. Furthermore, we demonstrate that supersymmetry is not a necessary requirement for a vanishing $a_{00} = N_f - N_b$, with models obeying this constraint appearing sporadically in the sample of models we analyse, and giving finite, non-vanishing cosmological constant. In Sections 5.1 and 5.2, we give an overview of how we constructed and analysed the partition function and potential of the fertile models at, and away from, the FFP, and how this relates to the Cosmological Constant. Finally, in Section 6 we present the statistics that result from the classification and in Section 7 we give an example of a model that fulfils

[¶]We remark that S -models contain both non-supersymmetric models, in which $N = 1$ spacetime supersymmetry is broken by a GGSO phase, and the supersymmetric models, in which the \mathbf{S} basis vector is the spacetime supersymmetry generator [19]

all fertility criteria and sits at a minima in potential close to, but not at, the FFP. Section 8 concludes this work with discussion of the results and prospective future work.

2 The $\tilde{\mathcal{S}}$ -Models

The FFF builds a models spectrum up from a set of basis vectors. These basis vectors enforce boundary conditions on a set of world sheet fermionic degrees of freedom, used to cancel the conformal anomaly. The second ingredient in this formalism are the phases between basis vectors, given by a generalised GSO (GGSO) matrix. This method has been used to build toy models, corresponding to $\mathbb{Z}_2 \times \mathbb{Z}_2$ orbifolds of 6 dimensional tori, for decades and has led to such discoveries as spinor-vector duality[31]. Here we employ it to sample the space of non-supersymmetric vacua and classify the solutions phenomenologically. Firstly we will define our basis vectors, determining the configuration of the world sheet fermions in each sector. The following vectors are adapted from the $SO(10)$ classification basis [32] by implementing the $\mathcal{S} \rightarrow \tilde{\mathcal{S}}$ map [21] and define our $\tilde{\mathcal{S}}$ -models in four dimensions.

$$\begin{aligned}
\mathbb{1} = \mathbf{v}_1 &= \{\psi^\mu, \chi^{1,\dots,6}, y^{1,\dots,6}, w^{1,\dots,6} \mid \bar{y}^{1,\dots,6}, \bar{w}^{1,\dots,6}, \bar{\eta}^{1,2,3}, \bar{\psi}^{1,\dots,5}, \bar{\phi}^{1,\dots,8}\} \\
\tilde{\mathcal{S}} = \mathbf{v}_2 &= \{\psi^\mu, \chi^{1,2}, \chi^{3,4}, \chi^{5,6} \mid \bar{\phi}^{3,4,5,6}\} \\
\mathbf{e}_i = \mathbf{v}_{2+i} &= \{y^i, w^i \mid \bar{y}^i, \bar{w}^i\} \quad \text{for } i = 1, 2, 3, 4, 5, 6 \\
\mathbf{b}_1 = \mathbf{v}_9 &= \{\psi^\mu, \chi^{1,2}, y^{3,4,5,6} \mid \bar{y}^{3,4,5,6}, \bar{\eta}^1, \bar{\psi}^{1,2,3,4,5}\} \\
\mathbf{b}_2 = \mathbf{v}_{10} &= \{\psi^\mu, \chi^{3,4}, y^{1,2}, w^{5,6} \mid \bar{y}^{1,2}, \bar{w}^{5,6}, \bar{\eta}^2, \bar{\psi}^{1,2,3,4,5}\} \\
\mathbf{z}_1 = \mathbf{v}_{11} &= \{\bar{\phi}^{1,2,3,4}\} \\
\mathbf{z}_2 = \mathbf{v}_{12} &= \{\bar{\phi}^{5,6,7,8}\}
\end{aligned} \tag{2.1}$$

Here, ψ^μ are the fermionic superpartners of the left-moving spacetime bosonic coordinates in the light-cone gauge; $\chi^{1,\dots,6}$ are the fermionic superpartners of the 6 dimensional left-moving compactified coordinates, y^i, w^i ; \bar{y}^i, \bar{w}^i correspond to the 6 right-moving internal, fermionised coordinates; and $\bar{\eta}^{1,2,3}$, $\bar{\psi}^{1,2,3,4,5}$, and $\bar{\phi}^{1,2,3,4,5,6,7,8}$ are 16 right-moving complex fermions required to cancel the conformal anomaly.

Considering the basis vectors: $\mathbb{1}$ is required for consistency; \mathbf{e}_i relate to shifts in the six dimensional compactified torus [32, 33, 30]; \mathbf{b}_a relate to $\mathbb{Z}_2 \times \mathbb{Z}_2$ orbifold twists; and \mathbf{z}_a relate to hidden sector gauge group breaking and enhancements, where $a = 1, 2$.

However the defining feature of this model is the modification of the spacetime supersymmetry generating vector $\mathcal{S} \rightarrow \tilde{\mathcal{S}}$,

$$\mathcal{S} = \{\psi^\mu, \chi^{1,2}, \chi^{3,4}, \chi^{5,6}\} \rightarrow \tilde{\mathcal{S}} = \{\psi^\mu, \chi^{1,2}, \chi^{3,4}, \chi^{5,6} \mid \bar{\phi}^{3,4,5,6}\} \tag{2.2}$$

with the $\tilde{\mathcal{S}}$ vector removing supersymmetry from the model at the ten dimensional level, eliminating the massless gravitinos found in similar \mathcal{S} -models. This mapping eliminates the need for a spontaneous supersymmetry breaking mechanism, and alters the structure of the model significantly.

Having defined our basis vectors, the features of the model now depend only on the GGSO matrix with components $C \begin{bmatrix} \mathbf{v}_i \\ \mathbf{v}_j \end{bmatrix} = \pm 1$, from which we construct the Hilbert Space

of the model,

$$\mathcal{H} = \oplus \prod_{i=1}^k \{e^{i\pi v_i F_\alpha} |S_\alpha\rangle = \delta_\alpha C \begin{bmatrix} \mathbf{v}_i \\ \mathbf{v}_j \end{bmatrix}^* |S_\alpha\rangle\}. \quad (2.3)$$

where v_i are the basis vectors, α labels the sector, F_α is the fermion number operator, and δ_α is the spin statistics index, equal to ± 1 .

Sectors, $|S_\alpha\rangle$, are constructed from linear combinations of the basis vectors (addition modulo 2) and are described by their mass. The left and right moving components of the mass are:

$$\mathcal{M}_L^2 = -\frac{1}{2} + \frac{\alpha_L \cdot \alpha_L}{8} + N_L \quad (2.4)$$

$$\mathcal{M}_R^2 = -1 + \frac{\alpha_R \cdot \alpha_R}{8} + N_R, \quad (2.5)$$

where N_L, N_R sum over the left- and right-moving oscillators. Physical states satisfy the Virasoro level-matching condition $\mathcal{M}_L^2 = \mathcal{M}_R^2$

As the entries above the diagonal of the 12×12 GGSO matrix are free parameters, taking values of ± 1 , a space of 2^{66} potential GGSO matrices describe $2^{66} \approx 10^{20}$ potential models. Only a fraction of these will be phenomenologically viable. The following sections detail the conditions on the GGSO matrix elements required for states to remain in the model. Randomly sampling GGSO matrices allows us to find the frequency of models that satisfy the conditions.

3 Analysis of Tachyonic Sectors

Tachyonic states with negative level-matched mass squared, $\mathcal{M}_L^2 = \mathcal{M}_R^2 = \mathcal{M}^2 < 0$, indicate the model lies on a maximum of the potential. In order to ensure that we find models that are phenomenologically viable and stable, we use the condition that all level-matched tachyons are projected from the spectrum, though tachyonic models that are stable can be constructed [34]. In this regard the sample could be considered to be overly constricted, however these conditions follow the precedent set in the literature [21, 22, 35] and are chosen such that comparison to S -models is convenient. Without employing supersymmetry to stabilise our model, each tachyonic state must be accounted for and projected individually. A detailed review of the tachyonic sectors and their mass levels is given in [21], which analyses a similar \tilde{S} -model, but with a slightly different basis set. For completeness, the on shell tachyons are defined in Table 1. Similarly, examples of the survival conditions of the tachyonic sectors are given in Table 2 and Table 3. These conditions are derived from eq. (2.3). A key feature of this model is the relationship between the tachyonic states and the observable enhancements. In particular the survival conditions for the $|z_{1,2}\rangle$ tachyonic states are the same as those for the $\psi^\mu \bar{\psi}^{1,\dots,5(*)} |z_{1,2}\rangle$ enhancements to the gauge group. Therefore, for this choice of basis vectors, there are no tachyon free models with an enhanced $SO(10)$ symmetry. This is discussed further in Subsection 4.6.

As demonstrated in Tables 2 and 3, the spinorial tachyons have slightly simpler conditions for survival than their vectorial counterpart, and this is due to the presence of the oscillator. All possible oscillators must be accounted for and projected. Once all 126 possible tachyonic states have been projected, we can build up the massless spectrum.

Mass level	Vectorial States	Spinorial States
$(-\frac{1}{2}, -\frac{1}{2})$	$\bar{\lambda}_m \mathbf{0}\rangle$	$ \mathbf{z}_{1,2}\rangle$
$(-\frac{3}{8}, -\frac{3}{8})$	$\bar{\lambda}_m \mathbf{e}_i\rangle$	$ \mathbf{e}_i + \mathbf{z}_{1,2}\rangle$
$(-\frac{1}{4}, -\frac{1}{4})$	$\bar{\lambda}_m \mathbf{e}_i + \mathbf{e}_j\rangle$	$ \mathbf{e}_i + \mathbf{e}_j + \mathbf{z}_{1,2}\rangle$
$(-\frac{1}{8}, -\frac{1}{8})$	$\bar{\lambda}_m \mathbf{e}_i + \mathbf{e}_j + \mathbf{e}_k\rangle$	$ \mathbf{e}_i + \mathbf{e}_j + \mathbf{e}_k + \mathbf{z}_{1,2}\rangle$

Table 1: Level-matched tachyonic states and their corresponding mass level, with $i \neq j \neq k = 1, \dots, 6$ and $\bar{\lambda}_m$ being any right-moving complimentary fermion oscillator

Spinorial State	Survival Condition						
\mathbf{z}_1	C	$\begin{array}{ c } \hline \mathbf{z}_1 \\ \hline \mathbf{e}_{1,\dots,6} \\ \hline \end{array}$	$= C$	$\begin{array}{ c } \hline \mathbf{z}_1 \\ \hline \mathbf{b}_{1,2} \\ \hline \end{array}$	$= C$	$\begin{array}{ c } \hline \mathbf{z}_1 \\ \hline \mathbf{z}_2 \\ \hline \end{array}$	$= +1$
\mathbf{z}_2	C	$\begin{array}{ c } \hline \mathbf{z}_2 \\ \hline \mathbf{e}_{1,\dots,6} \\ \hline \end{array}$	$= C$	$\begin{array}{ c } \hline \mathbf{z}_2 \\ \hline \mathbf{b}_{1,2} \\ \hline \end{array}$	$= C$	$\begin{array}{ c } \hline \mathbf{z}_2 \\ \hline \mathbf{z}_1 \\ \hline \end{array}$	$= +1$
$\mathbf{e}_1 + \mathbf{z}_1$	C	$\begin{array}{ c } \hline \mathbf{e}_1 + \mathbf{z}_1 \\ \hline \mathbf{e}_{2,\dots,6} \\ \hline \end{array}$	$= C$	$\begin{array}{ c } \hline \mathbf{e}_1 + \mathbf{z}_1 \\ \hline \mathbf{b}_1 \\ \hline \end{array}$	$= C$	$\begin{array}{ c } \hline \mathbf{e}_1 + \mathbf{z}_1 \\ \hline \mathbf{z}_2 \\ \hline \end{array}$	$= +1$
$\mathbf{e}_1 + \mathbf{z}_2$	C	$\begin{array}{ c } \hline \mathbf{e}_1 + \mathbf{z}_2 \\ \hline \mathbf{e}_{2,\dots,6} \\ \hline \end{array}$	$= C$	$\begin{array}{ c } \hline \mathbf{e}_1 + \mathbf{z}_2 \\ \hline \mathbf{b}_1 \\ \hline \end{array}$	$= C$	$\begin{array}{ c } \hline \mathbf{e}_1 + \mathbf{z}_2 \\ \hline \mathbf{z}_1 \\ \hline \end{array}$	$= +1$
$\mathbf{e}_1 + \mathbf{e}_2 + \mathbf{z}_1$	C	$\begin{array}{ c } \hline \mathbf{e}_1 + \mathbf{e}_2 + \mathbf{z}_1 \\ \hline \mathbf{e}_{3,\dots,6} \\ \hline \end{array}$	$= C$	$\begin{array}{ c } \hline \mathbf{e}_1 + \mathbf{e}_2 + \mathbf{z}_1 \\ \hline \mathbf{b}_1 \\ \hline \end{array}$	$= C$	$\begin{array}{ c } \hline \mathbf{e}_1 + \mathbf{e}_2 + \mathbf{z}_1 \\ \hline \mathbf{z}_2 \\ \hline \end{array}$	$= +1$
$\mathbf{e}_1 + \mathbf{e}_2 + \mathbf{z}_2$	C	$\begin{array}{ c } \hline \mathbf{e}_1 + \mathbf{e}_2 + \mathbf{z}_2 \\ \hline \mathbf{e}_{3,\dots,6} \\ \hline \end{array}$	$= C$	$\begin{array}{ c } \hline \mathbf{e}_1 + \mathbf{e}_2 + \mathbf{z}_2 \\ \hline \mathbf{b}_1 \\ \hline \end{array}$	$= C$	$\begin{array}{ c } \hline \mathbf{e}_1 + \mathbf{e}_2 + \mathbf{z}_2 \\ \hline \mathbf{z}_1 \\ \hline \end{array}$	$= +1$
$\mathbf{e}_1 + \mathbf{e}_2 + \mathbf{e}_3 + \mathbf{z}_1$	C	$\begin{array}{ c } \hline \mathbf{e}_1 + \mathbf{e}_2 + \mathbf{e}_3 + \mathbf{z}_1 \\ \hline \mathbf{e}_{4,5,6} \\ \hline \end{array}$	$= C$	$\begin{array}{ c } \hline \mathbf{e}_1 + \mathbf{e}_2 + \mathbf{e}_3 + \mathbf{z}_1 \\ \hline \mathbf{z}_2 \\ \hline \end{array}$	$= C$	$\begin{array}{ c } \hline \mathbf{e}_1 + \mathbf{e}_2 + \mathbf{e}_3 + \mathbf{z}_1 \\ \hline \mathbf{z}_2 \\ \hline \end{array}$	$= +1$
$\mathbf{e}_1 + \mathbf{e}_2 + \mathbf{e}_3 + \mathbf{z}_2$	C	$\begin{array}{ c } \hline \mathbf{e}_1 + \mathbf{e}_2 + \mathbf{e}_3 + \mathbf{z}_2 \\ \hline \mathbf{e}_{4,5,6} \\ \hline \end{array}$	$= C$	$\begin{array}{ c } \hline \mathbf{e}_1 + \mathbf{e}_2 + \mathbf{e}_3 + \mathbf{z}_2 \\ \hline \mathbf{z}_1 \\ \hline \end{array}$	$= C$	$\begin{array}{ c } \hline \mathbf{e}_1 + \mathbf{e}_2 + \mathbf{e}_3 + \mathbf{z}_2 \\ \hline \mathbf{z}_1 \\ \hline \end{array}$	$= +1$

Table 2: Level-matched tachyonic spinorial states and the survival conditions of their GGSO Coefficients. This is not an exhaustive list and analogous conditions were found for other combinations of \mathbf{e}_i .

Vectorial State	$C \begin{bmatrix} \mathbf{e}_1 \\ \tilde{\mathbf{S}} \end{bmatrix}$	$C \begin{bmatrix} \mathbf{e}_1 \\ \mathbf{e}_2 \end{bmatrix}$	$C \begin{bmatrix} \mathbf{e}_1 \\ \mathbf{e}_3 \end{bmatrix}$	$C \begin{bmatrix} \mathbf{e}_1 \\ \mathbf{e}_4 \end{bmatrix}$	$C \begin{bmatrix} \mathbf{e}_1 \\ \mathbf{e}_5 \end{bmatrix}$	$C \begin{bmatrix} \mathbf{e}_1 \\ \mathbf{e}_6 \end{bmatrix}$	$C \begin{bmatrix} \mathbf{e}_1 \\ \mathbf{b}_1 \end{bmatrix}$	$C \begin{bmatrix} \mathbf{e}_1 \\ \mathbf{z}_1 \end{bmatrix}$	$C \begin{bmatrix} \mathbf{e}_1 \\ \mathbf{z}_2 \end{bmatrix}$
$\bar{y}_2 \mathbf{e}_1\rangle$	+	-	+	+	+	+	-	+	+
$\bar{y}_3 \mathbf{e}_1\rangle$	+	+	-	+	+	+	-	+	+
$\bar{y}_4 \mathbf{e}_1\rangle$	+	+	+	-	+	+	-	+	+
$\bar{y}_5 \mathbf{e}_1\rangle$	+	+	+	+	-	+	-	+	+
$\bar{y}_6 \mathbf{e}_1\rangle$	+	+	+	+	+	-	-	+	+
$\bar{w}_2 \mathbf{e}_1\rangle$	+	-	+	+	+	+	+	+	+
$\bar{w}_3 \mathbf{e}_1\rangle$	+	+	-	+	+	+	+	+	+
$\bar{w}_4 \mathbf{e}_1\rangle$	+	+	+	-	+	+	+	+	+
$\bar{w}_5 \mathbf{e}_1\rangle$	+	+	+	+	-	+	+	+	+
$\bar{w}_6 \mathbf{e}_1\rangle$	+	+	+	+	+	-	+	+	+
$\psi^{1,\dots,5(*)}/\eta^{1(*)} \mathbf{e}_1\rangle$	+	+	+	+	+	+	-	+	+
$\eta^{2,3(*)} \mathbf{e}_1\rangle$	+	+	+	+	+	+	+	+	+
$\phi^{1,2(*)} \mathbf{e}_1\rangle$	+	+	+	+	+	+	+	-	+
$\phi^{3,4(*)} \mathbf{e}_1\rangle$	-	+	+	+	+	+	+	-	+
$\phi^{5,6(*)} \mathbf{e}_1\rangle$	-	+	+	+	+	+	+	+	-
$\phi^{7,8(*)} \mathbf{e}_1\rangle$	+	+	+	+	+	+	+	+	-

Table 3: Level-matched tachyonic vectorial states and the survival conditions of their GGSO Coefficients. This is not an exhaustive list but demonstrates the trend.

4 Analysis of Massless Sectors

Having removed level-matched tachyonic states from the spectrum, we can turn our attention to the massless states. It is from these states that we can build our $SO(10)$ GUT model, and so we must ensure that they are compatible with the observed SM data. The key states we will look for are the fermion producing spinorial $\mathbf{16}/\overline{\mathbf{16}}$ representations, and the boson producing vectorial $\mathbf{10}$ representations.

4.1 Spinorials

The spinorial $\mathbf{16}/\overline{\mathbf{16}}$ representation of $SO(10)$ appear as the following 48 states:

$$\begin{aligned} \mathbf{F}_{pqrs}^{(1)} &= \mathbf{b}_1 + p\mathbf{e}_3 + q\mathbf{e}_4 + r\mathbf{e}_5 + s\mathbf{e}_6 \\ &= \{\psi^\mu, \chi^{1,2}, (1-p)y^3\bar{y}^3, pw^3\bar{w}^3, (1-q)y^4\bar{y}^4, qw^4\bar{w}^4, \\ &\quad (1-r)y^5\bar{y}^5, rw^5\bar{w}^5, (1-s)y^6\bar{y}^6, sw^6\bar{w}^6, \bar{\eta}^1, \bar{\psi}^{1,\dots,5}\} \end{aligned} \quad (4.1)$$

$$\mathbf{F}_{pqrs}^{(2)} = \mathbf{b}_2 + p\mathbf{e}_1 + q\mathbf{e}_2 + r\mathbf{e}_5 + s\mathbf{e}_6 \quad (4.2)$$

$$\mathbf{F}_{pqrs}^{(3)} = \mathbf{b}_3 + p\mathbf{e}_1 + q\mathbf{e}_2 + r\mathbf{e}_3 + s\mathbf{e}_4 \quad (4.3)$$

where $pqrs = 0, 1$. Here the vector \mathbf{b}_3 is constructed from the following basis vectors:

$$\begin{aligned} \mathbf{b}_3 &= \mathbf{1} + \mathbf{b}_1 + \mathbf{b}_2 + \mathbf{z}_1 + \mathbf{z}_2 \\ &= \{\psi^\mu, \chi^{5,6}, w^{1,2}, w^{3,4}|\bar{w}^{1,2}, \bar{w}^{3,4}, \eta^3\bar{\psi}^{1,\dots,5}\} \end{aligned} \quad (4.4)$$

In order to count the number of $\mathbf{16}/\overline{\mathbf{16}}$ in the model, we can define the projectors, $P_{pqrs}^{(i)}$, and the chiral phases, $X_{pqrs}^{(i)}$, of each of these states. The projectors for these sectors are as follows:

$$P_{pqrs}^{(1)} = \frac{1}{2^4} \prod_{i=1,2} \left(1 - C \left[\begin{array}{c} \mathbf{F}_{pqrs}^{(1)} \\ \mathbf{e}_i \end{array} \right]^* \right) \prod_{a=1,2} \left(1 - C \left[\begin{array}{c} \mathbf{F}_{pqrs}^{(1)} \\ \mathbf{z}_a \end{array} \right]^* \right) \quad (4.5)$$

$$P_{pqrs}^{(2)} = \frac{1}{2^4} \prod_{i=3,4} \left(1 - C \left[\begin{array}{c} \mathbf{F}_{pqrs}^{(2)} \\ \mathbf{e}_i \end{array} \right]^* \right) \prod_{a=1,2} \left(1 - C \left[\begin{array}{c} \mathbf{F}_{pqrs}^{(2)} \\ \mathbf{z}_a \end{array} \right]^* \right) \quad (4.6)$$

$$P_{pqrs}^{(3)} = \frac{1}{2^4} \prod_{i=5,6} \left(1 - C \left[\begin{array}{c} \mathbf{F}_{pqrs}^{(3)} \\ \mathbf{e}_i \end{array} \right]^* \right) \prod_{a=1,2} \left(1 - C \left[\begin{array}{c} \mathbf{F}_{pqrs}^{(3)} \\ \mathbf{z}_a \end{array} \right]^* \right) \quad (4.7)$$

Similarly, the chiral phases are the following:

$$X_{pqrs}^{(1)} = -C \left[\begin{array}{c} \mathbf{F}_{pqrs}^{(1)} \\ \mathbf{b}_2 + r\mathbf{e}_5 + s\mathbf{e}_6 \end{array} \right]^* \quad (4.8)$$

$$X_{pqrs}^{(2)} = -C \left[\begin{array}{c} \mathbf{F}_{pqrs}^{(2)} \\ \mathbf{b}_1 + r\mathbf{e}_5 + s\mathbf{e}_6 \end{array} \right]^* \quad (4.9)$$

$$X_{pqrs}^{(3)} = -C \left[\begin{array}{c} \mathbf{F}_{pqrs}^{(3)} \\ \mathbf{b}_1 + r\mathbf{e}_3 + s\mathbf{e}_4 \end{array} \right]^* \quad (4.10)$$

From these, we can determine the numbers N_{16} and $N_{\overline{16}}$ of $\mathbf{16}/\overline{\mathbf{16}}$ $SO(10)$ representations,

$$N_{16} = \frac{1}{2} \sum_{\substack{A=1,2,3 \\ pqrs=0,1}} P_{pqrs}^A (1 + X_{pqrs}^A) \quad (4.11)$$

$$N_{\overline{16}} = \frac{1}{2} \sum_{\substack{A=1,2,3 \\ pqrs=0,1}} P_{pqrs}^A (1 - X_{pqrs}^A) \quad (4.12)$$

To ensure the model is compatible with the 3 generational SM, we must enforce the constraint:

$$N_{16} - N_{\overline{16}} \geq 6 \quad (4.13)$$

This ensures that the model has 6 or more chiral generations at the $SO(10)$ level and is a necessary but not sufficient condition on the presence of three generations at the subgroup level. For example, additional basis vectors are required to break to the group down to Pati–Salam [36, 37, 38] or Standard–like Models [1, 2, 39] and their projection conditions will determine whether 3 chiral generations remain in the spectrum. We remark that Pati–Salam \tilde{S} –models are not viable due to the absence from the spectrum of the heavy Higgs states required to break the Pati–Salam symmetry down to the Standard Model, whereas the Standard–like \tilde{S} –models may be viable [22]. In contrast to the supersymmetric S –Models, there are no bosonic superpartners to these spinorial $\mathbf{16}/\overline{\mathbf{16}}$ ’s. In particular, adding $\tilde{\mathbf{S}}$ to $\mathbf{F}_{pqrs}^{(i)}$ states produces massive states coupled to the hidden sector. We note that in the free fermionic heterotic–string models with an unbroken GUT symmetry, these sectors give rise to the heavy Higgs states that are used to break the GUT symmetry.

4.2 Vectorials

To map from the spinorial to the vectorial sectors, we define the vector $\tilde{\mathbf{x}}$

$$\begin{aligned}\tilde{\mathbf{x}} &= \sum_{i=1,2,3} \mathbf{b}_i + \sum_{a=1,2,3,4,5,6} \mathbf{e}_i \\ &= \{\psi^\mu, \chi^{1,2,3,4,5,6} \mid \bar{\eta}^{1,2,3}, \bar{\psi}^{1,\dots,5}\}.\end{aligned}\tag{4.14}$$

This sector maps the spacetime fermions in the spinorial $\mathbf{16}/\overline{\mathbf{16}}$ representation of $SO(10)$ to sectors that produce spacetime bosons in its vectorial representation. In other words SM matter particle states map to the Standard Model Higgs-compatible states.

The vectorial $\mathbf{10}$ representation of $SO(10)$ is produced from the oscillators $\bar{\psi}^{a=1,\dots,5(*)}$ acting in the sectors given by

$$\begin{aligned}\mathbf{V}_{pqrs}^{(1)} &= \mathbf{F}_{pqrs}^{(1)} + \tilde{\mathbf{x}} \\ &= \mathbf{b}_2 + \mathbf{b}_3 + p\mathbf{e}_3 + q\mathbf{e}_4 + r\mathbf{e}_5 + s\mathbf{e}_6 \\ &= \{\chi^{3,4}, \chi^{5,6}, (1-p)y^3\bar{y}^3, pw^3\bar{w}^3, (1-q)y^4\bar{y}^4, qw^4\bar{w}^4, \\ &\quad (1-r)y^5\bar{y}^5, rw^5\bar{w}^5, (1-s)y^6\bar{y}^6, sw^6\bar{w}^6, \bar{\eta}^{2,3}\}\end{aligned}\tag{4.15}$$

$$\mathbf{V}_{pqrs}^{(2)} = \mathbf{F}_{pqrs}^{(2)} + \tilde{\mathbf{x}}\tag{4.16}$$

$$\mathbf{V}_{pqrs}^{(3)} = \mathbf{F}_{pqrs}^{(3)} + \tilde{\mathbf{x}}\tag{4.17}$$

Again we can define projectors, $R_{pqrs}^{(i)}$, to determine if these states remain in the spectrum

$$R_{pqrs}^{(1)} = \frac{1}{2^4} \prod_{i=1,2} \left(1 + C \left[\mathbf{V}_{pqrs}^{(1)} \right]^*\right) \prod_{a=1,2} \left(1 + C \left[\mathbf{z}_a \right]^*\right)\tag{4.18}$$

$$R_{pqrs}^{(2)} = \frac{1}{2^4} \prod_{i=3,4} \left(1 + C \left[\mathbf{V}_{pqrs}^{(2)} \right]^*\right) \prod_{a=1,2} \left(1 + C \left[\mathbf{z}_a \right]^*\right)\tag{4.19}$$

$$R_{pqrs}^{(3)} = \frac{1}{2^4} \prod_{i=5,6} \left(1 + C \left[\mathbf{V}_{pqrs}^{(3)} \right]^*\right) \prod_{a=1,2} \left(1 + C \left[\mathbf{z}_a \right]^*\right)\tag{4.20}$$

and the number N_{10} that remain can be written as

$$N_{10} = \sum_{\substack{A=1,2,3 \\ pqrs=0,1}} R_{pqrs}^A.\tag{4.21}$$

To make our model compatible with the SM Higgs, we must ensure that at least one vectorial state remains that can produce the Higgs doublet

$$N_{10} \geq 1.\tag{4.22}$$

4.3 Hidden Sectors

Additional massless sectors will also contribute to the spectrum and partition function. A consequence of the $\tilde{\mathbf{S}}$ mapping is the production of large numbers of massless hidden sectors. These other massless groups take the general form:

$$\mathbf{H}_{pqrs}^{a,b,c,d} = V_{pqrs}^{(a)} + b\mathbf{z}_1 + c\mathbf{z}_2 + d\tilde{\mathbf{S}}\tag{4.23}$$

In particular the following 96 spinorial sectors will give rise to spacetime bosons:

$$\mathbf{H}_{pqrs}^{(a),(i)} = V_{pqrs}^{(a)} + \mathbf{z}_i \quad (4.24)$$

And the 192 following sectors giving hidden spacetime fermions:

$$\mathbf{H}_{pqrs}^{a,b,c,1} = V_{pqrs}^{(a)} + b\mathbf{z}_1 + c\mathbf{z}_2 + \tilde{\mathbf{S}} \quad (4.25)$$

with $a = 1, 2, 3$, $b, c, d = 0, 1$, $pqrs = 0, 1$ and $i = 1, 2$. The presence or absence of these hidden sectors will effect the constant (massless) term in the partition function q expansion and so has an effect on the cosmological constant of the model. Similarly, the vectors $\delta^{1,\dots,30}$ contribute 30 hidden sectors which do not fit into the general structure given in eq. (4.23).

$$\delta^{1,\dots,30} = \mathbf{e}_i + \mathbf{e}_j + \mathbf{e}_k + \mathbf{e}_l + \mathbf{z}_a \quad (4.26)$$

where $i \neq j \neq k \neq l = 1, \dots, 6$ and $a = 1, 2$.

4.4 Other Massless States

As the entire massless spectrum contributes to the partition function and potential, we briefly describe other contributions to the massless spectrum, which come in the following forms:

$$\gamma^{1,\dots,15} = \mathbf{e}_i + \mathbf{e}_j + \mathbf{e}_k + \mathbf{e}_l \quad (4.27)$$

$$\tilde{\mathbf{V}} = \tilde{\mathbf{S}} + b\mathbf{z}_1 + c\mathbf{z}_2 \quad (4.28)$$

where $i \neq j \neq k \neq l$, and $b, c = 0, 1$

The $\tilde{\mathbf{x}}$ sector given in eq. (4.14) will contribute to the observable sector in the form of additional $\mathbf{16}/\overline{\mathbf{16}}$ spinorial representations of the $SO(10)$. Both $\gamma^{1,\dots,15}$ and $\tilde{\mathbf{V}}$ produce vectorial representations. Considering $\gamma^{1,\dots,15}$, with oscillators $\bar{y}^i/\bar{w}^i/\bar{\eta}^{1,2,3}/\bar{\phi}^{1,\dots,8}$ these states are hidden sector states, however if the state has oscillator $\bar{\psi}^{1,\dots,5}$ these states will give vectorial $\mathbf{10}$ states. Similarly, when $\tilde{\mathbf{V}}$ states have y^i/w^i oscillators, the states contribute to the hidden sector, however if the oscillator is $\bar{\psi}^{1,\dots,5}/\bar{\eta}^{1,2,3}/\bar{\phi}^{1,\dots,8}$, with only complimentary NS $\bar{\phi}$ fermions, these states couple to both hidden and observable sectors. The vector-like states from these sectors can decouple from the chiral low scale spectrum by giving Vacuum Expectation Values to some fields in the massless string spectrum. These states do not couple in the same way as the previous \mathbf{F}_{pqrs}^i and \mathbf{V}_{pqrs}^i , and so any compatible SM states will not be found in any of these additional massless states.

4.5 Top Quark Mass Coupling

So far none of the criteria implemented have anything to say about interaction terms of the theory. A minimum requirement for a SM compatible model is a mechanism to give mass to the heaviest fermion, the Top quark, by coupling it to the Higgs. In this respect we note that there are two types of couplings that can give rise to top quark mass term, which involves twisted T , and untwisted U , matter fields. The first coupling is of the form $T_i T_i U_i$ where $i = 1, 2, 3$ denotes the three twisted planes of the $\mathbb{Z}_2 \times \mathbb{Z}_2$ orbifolds. The second type of couplings is of the form $T_i T_j T_k$ with $i \neq j \neq k$. In the quasi-realistic models with unbroken Pati-Salam [37, 38], or Standard-like Model [1, 2, 39], $SO(10)$ subgroup there

exist a doublet–splitting mechanism [40] that depends on the assignment of symmetric versus anti–symmetric boundary conditions for the set of internal worldsheet fermions that correspond to the compactified toroidal dimensions. Symmetric boundary conditions give rise to untwisted colour triplets, whereas anti–symmetric boundary conditions give rise to electroweak doublets. Similarly, in vacua that contain a basis vector that breaks the $SO(10)$ symmetry to the flipped $SU(5)$ subgroup, there is a top–bottom quark Yukawa coupling selection rule [41], where for symmetric boundary conditions a bottom–quark $T_i T_i U_i$ Yukawa coupling is selected and for asymmetric boundary conditions a top–quark Yukawa coupling is selected. In this paper the $SO(10)$ symmetry is unbroken and in principle both type of couplings are obtained. Given that the models that we consider use symmetric boundary conditions, we impose the presence of the second type of couplings as a potential top quark mass term.

We impose that the Top Quark Mass Coupling (TQMC) must also be preserved through the following conditions, a detailed account of which is given in [42]. Preserving the TQMC requires us to fix certain GGSO phases, such that we retain two spinorial states and a Vectorial state (Higgs) that take part in this tree-level interaction. Without loss of generality we can choose the spinorials $\mathbf{F}_{0000}^{(1)} = \mathbf{b}_1$, $\mathbf{F}_{0000}^{(2)} = \mathbf{b}_2$ and vectorial $\mathbf{F}_{1111}^{(3)} + \tilde{\mathbf{x}} = b_3 + \mathbf{e}_1 + \mathbf{e}_2 + \mathbf{e}_3 + \mathbf{e}_4 + \tilde{\mathbf{x}}$. These states are chosen for ease of implementing the conditions. Having decided on the states, we find the following survival conditions:

$$C \begin{bmatrix} \mathbf{e}_i \\ \mathbf{b}_1 \end{bmatrix} = C \begin{bmatrix} \mathbf{z}_a \\ \mathbf{b}_1 \end{bmatrix} = -1 \text{ for } i = 1, 2 \text{ a} = 1, 2 \quad (4.29)$$

$$C \begin{bmatrix} \mathbf{e}_i \\ \mathbf{b}_2 \end{bmatrix} = C \begin{bmatrix} \mathbf{z}_a \\ \mathbf{b}_2 \end{bmatrix} = -1 \text{ for } i = 3, 4 \text{ a} = 1, 2 \quad (4.30)$$

$$C \begin{bmatrix} \mathbf{z}_i \\ \mathbf{b}_1 \end{bmatrix} C \begin{bmatrix} \mathbf{z}_i \\ \mathbf{b}_2 \end{bmatrix} C \begin{bmatrix} \mathbf{z}_i \\ \mathbf{e}_5 \end{bmatrix} C \begin{bmatrix} \mathbf{z}_i \\ \mathbf{e}_6 \end{bmatrix} = 1 \text{ for } i = 1, 2 \quad (4.31)$$

$$C \begin{bmatrix} \mathbf{e}_i \\ \mathbf{b}_1 \end{bmatrix} C \begin{bmatrix} \mathbf{e}_i \\ \mathbf{b}_2 \end{bmatrix} C \begin{bmatrix} \mathbf{e}_i \\ \mathbf{e}_5 \end{bmatrix} C \begin{bmatrix} \mathbf{e}_i \\ \mathbf{e}_6 \end{bmatrix} = 1 \text{ for } i = 5, 6 \quad (4.32)$$

$$C \begin{bmatrix} \mathbf{b}_1 \\ \mathbf{b}_2 \end{bmatrix} = C \begin{bmatrix} \mathbf{b}_2 \\ \mathbf{b}_1 \end{bmatrix} = -1 \quad (4.33)$$

Eq. (4.31) being somewhat redundant due to the previous tachyon projection conditions and eq. (4.29) and (4.30).

4.6 Enhancements

Gauge enhancements arise within this class of models from the sectors

$$\psi^\mu \{ \bar{\lambda}^i \} | \mathbf{z}_1 \rangle \quad (4.34)$$

$$\psi^\mu \{ \bar{\lambda}^i \} | \mathbf{z}_2 \rangle \quad (4.35)$$

$$\psi^\mu | \mathbf{z}_1 + \mathbf{z}_2 \rangle \quad (4.36)$$

where $\bar{\lambda}^i$ are all possible right–moving NS oscillators. Survival conditions for the $| \mathbf{z}_1 \rangle$ enhancements are listed in Table 4. The observable enhancements to the $SO(10)$ gauge group arise for $\bar{\lambda}^i = \bar{\psi}^{1, \dots, 5}$ in the above sectors. Comparing Tables 4 and 2, we see the survival conditions of these states are identical to the $| \mathbf{z}_i \rangle$ tachyonic states. Therefore these enhancements would necessarily be projected out when looking for stable models.

Enhancement	$C \begin{matrix} \mathbf{z}_1 \\ \mathbf{e}_1 \end{matrix}$	$C \begin{matrix} \mathbf{z}_1 \\ \mathbf{e}_2 \end{matrix}$	$C \begin{matrix} \mathbf{z}_1 \\ \mathbf{e}_3 \end{matrix}$	$C \begin{matrix} \mathbf{z}_1 \\ \mathbf{e}_4 \end{matrix}$	$C \begin{matrix} \mathbf{z}_1 \\ \mathbf{e}_5 \end{matrix}$	$C \begin{matrix} \mathbf{z}_1 \\ \mathbf{e}_6 \end{matrix}$	$C \begin{matrix} \mathbf{z}_1 \\ \mathbf{b}_1 \end{matrix}$	$C \begin{matrix} \mathbf{z}_1 \\ \mathbf{b}_2 \end{matrix}$	$C \begin{matrix} \mathbf{z}_1 \\ \mathbf{z}_2 \end{matrix}$
$\psi^\mu \bar{y}_1 \mathbf{z}_1 \rangle$	-	+	+	+	+	+	-	+	+
$\psi^\mu \bar{y}_2 \mathbf{z}_1 \rangle$	+	-	+	+	+	+	-	+	+
$\psi^\mu \bar{y}_3 \mathbf{z}_1 \rangle$	+	+	-	+	+	+	+	-	+
$\psi^\mu \bar{y}_4 \mathbf{z}_1 \rangle$	+	+	+	-	+	+	+	-	+
$\psi^\mu \bar{y}_5 \mathbf{z}_1 \rangle$	+	+	+	+	-	+	+	-	+
$\psi^\mu \bar{y}_6 \mathbf{z}_1 \rangle$	+	+	+	+	+	-	+	-	+
$\psi^\mu \bar{w}_1 \mathbf{z}_1 \rangle$	-	+	+	+	+	+	-	-	+
$\psi^\mu \bar{w}_2 \mathbf{z}_1 \rangle$	+	-	+	+	+	+	-	-	+
$\psi^\mu \bar{w}_3 \mathbf{z}_1 \rangle$	+	+	-	+	+	+	-	-	+
$\psi^\mu \bar{w}_4 \mathbf{z}_1 \rangle$	+	+	+	-	+	+	-	-	+
$\psi^\mu \bar{w}_5 \mathbf{z}_1 \rangle$	+	+	+	+	-	+	-	+	+
$\psi^\mu \bar{w}_6 \mathbf{z}_1 \rangle$	+	+	+	+	+	-	-	+	+
$\psi^\mu \psi^{1,\dots,5(*)} \mathbf{z}_1 \rangle$	+	+	+	+	+	+	+	+	+
$\psi^\mu \eta^{1(*)} \mathbf{z}_1 \rangle$	+	+	+	+	+	+	+	-	+
$\psi^\mu \eta^{2(*)} \mathbf{z}_1 \rangle$	+	+	+	+	+	+	-	+	+
$\psi^\mu \eta^{3(*)} \mathbf{z}_1 \rangle$	+	+	+	+	+	+	-	-	+
$\psi^\mu \phi^{5,6(*)} \mathbf{z}_1 \rangle$	+	+	+	+	+	+	-	-	-
$\psi^\mu \phi^{7,8(*)} \mathbf{z}_1 \rangle$	+	+	+	+	+	+	-	-	-

Table 4: Enhancements and the survival conditions of their GGSO Coefficients, for the $|\mathbf{z}_1\rangle$ enhancements. The conditions for observable enhancementets, $\psi^\mu \psi^{1,\dots,5(*)} | \mathbf{z}_1 \rangle$, are shown here to be the same as the condition for the tachyonic states.

4.7 $N_b - N_f = 0$ at the Massless Level

It is possible to find models in which $N_b = N_f$ at the massless level as one would have for supersymmetric models at the free fermionic point (FFP). These models will appear sporadically as there is no inbuilt mechanism to produce this phenomenon. This condition could also be achieved by moving away from the FFP in moduli space [43, 10, 11]. The typical motivation for this condition is in the context of ‘super no-scale’ models [44] where it plays a role in the exponential suppression of the one loop cosmological constant for models with spontaneous breaking of supersymmetry. Although the \tilde{S} -models exhibit explicit breaking of supersymmetry this Bose-Fermi degeneracy at the massless level is still an interesting feature of the spectrum to note due to its analogy to supersymmetric models.

5 Partition Function and Potential

5.1 Partition Function

The partition function of a string model expresses information about the full tower of string states, both on-shell and off-shell. In particular, when written as a q -expansion, the total number of states at each mass can be read off. For example, the coefficient $a_{00} = N_b - N_f$ gives the net number of bosons and fermions at the massless level and so is necessarily 0 in supersymmetric models. For non-supersymmetric models we typically get a much richer spectrum with $a_{ij} \neq 0$. One feature to emphasize is the off-shell tachyon contributions, including the model-independent ‘proto-graviton’ state as demonstrated in ref. [45].

In the FFF, the partition function can be expressed as

$$Z = Z_B \sum_{\alpha, \beta} C \begin{bmatrix} \alpha \\ \beta \end{bmatrix} \prod_f Z \begin{bmatrix} \alpha(f) \\ \beta(f) \end{bmatrix} \quad (5.1)$$

where α and β are sectors, the product is over the fermion boundary conditions in each sector and Z_B is the spacetime boson contribution. However, it is more convenient to express the partition function in the following modular invariant way, as outlined in [32, 33, 11, 30, 46]:

$$\begin{aligned} Z = & \frac{1}{\eta^{12} \bar{\eta}^{24}} \frac{1}{2^3} \sum_{\substack{a, k, \rho \\ b, l, \sigma}} \frac{1}{2^6} \sum_{\substack{\zeta_i \\ \delta_i}} \frac{1}{2^3} \sum_{\substack{h_1, h_2, H \\ g_1, g_2, G}} (-1)^{a+b+\phi} \begin{bmatrix} a & k & \rho & \zeta_i & h_1 & h_2 & H \\ b & l & \sigma & \delta_i & g_1 & g_2 & G \end{bmatrix} \\ & \vartheta \begin{bmatrix} a \\ b \end{bmatrix}_{\psi^\mu} \vartheta \begin{bmatrix} a + h_2 \\ b + g_2 \end{bmatrix}_{\chi^{1,2}} \vartheta \begin{bmatrix} a + h_1 \\ b + g_1 \end{bmatrix}_{\chi^{3,4}} \vartheta \begin{bmatrix} a - h_1 - h_2 \\ b - g_1 - g_2 \end{bmatrix}_{\chi^{5,6}} \\ & \vartheta \begin{bmatrix} \zeta_1 \\ \delta_1 \end{bmatrix}_{w^1}^{\frac{1}{2}} \vartheta \begin{bmatrix} \zeta_1 + h_2 \\ \delta_1 + g_2 \end{bmatrix}_{y^1}^{\frac{1}{2}} \bar{\vartheta} \begin{bmatrix} \zeta_1 \\ \delta_1 \end{bmatrix}_{\bar{w}^1}^{\frac{1}{2}} \bar{\vartheta} \begin{bmatrix} \zeta_1 + h_2 \\ \delta_1 + g_2 \end{bmatrix}_{\bar{y}^1}^{\frac{1}{2}} \\ & \vartheta \begin{bmatrix} \zeta_2 \\ \delta_2 \end{bmatrix}_{w^2}^{\frac{1}{2}} \vartheta \begin{bmatrix} \zeta_2 + h_2 \\ \delta_2 + g_2 \end{bmatrix}_{y^2}^{\frac{1}{2}} \bar{\vartheta} \begin{bmatrix} \zeta_2 \\ \delta_2 \end{bmatrix}_{\bar{w}^2}^{\frac{1}{2}} \bar{\vartheta} \begin{bmatrix} \zeta_2 + h_2 \\ \delta_2 + g_2 \end{bmatrix}_{\bar{y}^2}^{\frac{1}{2}} \\ & \vartheta \begin{bmatrix} \zeta_3 \\ \delta_3 \end{bmatrix}_{w^3}^{\frac{1}{2}} \vartheta \begin{bmatrix} \zeta_3 + h_1 \\ \delta_3 + g_1 \end{bmatrix}_{y^3}^{\frac{1}{2}} \bar{\vartheta} \begin{bmatrix} \zeta_3 \\ \delta_3 \end{bmatrix}_{\bar{w}^3}^{\frac{1}{2}} \bar{\vartheta} \begin{bmatrix} \zeta_3 + h_1 \\ \delta_3 + g_1 \end{bmatrix}_{\bar{y}^3}^{\frac{1}{2}} \\ & \vartheta \begin{bmatrix} \zeta_4 \\ \delta_4 \end{bmatrix}_{w^4}^{\frac{1}{2}} \vartheta \begin{bmatrix} \zeta_4 + h_1 \\ \delta_4 + g_1 \end{bmatrix}_{y^4}^{\frac{1}{2}} \bar{\vartheta} \begin{bmatrix} \zeta_4 \\ \delta_4 \end{bmatrix}_{\bar{w}^4}^{\frac{1}{2}} \bar{\vartheta} \begin{bmatrix} \zeta_4 + h_1 \\ \delta_4 + g_1 \end{bmatrix}_{\bar{y}^4}^{\frac{1}{2}} \\ & \vartheta \begin{bmatrix} \zeta_5 + h_2 \\ \delta_5 + g_2 \end{bmatrix}_{w^5}^{\frac{1}{2}} \vartheta \begin{bmatrix} \zeta_5 + h_1 \\ \delta_5 + g_1 \end{bmatrix}_{y^5}^{\frac{1}{2}} \bar{\vartheta} \begin{bmatrix} \zeta_5 + h_2 \\ \delta_5 + g_2 \end{bmatrix}_{\bar{w}^5}^{\frac{1}{2}} \bar{\vartheta} \begin{bmatrix} \zeta_5 + h_1 \\ \delta_5 + g_1 \end{bmatrix}_{\bar{y}^5}^{\frac{1}{2}} \\ & \vartheta \begin{bmatrix} \zeta_6 + h_2 \\ \delta_6 + g_2 \end{bmatrix}_{w^6}^{\frac{1}{2}} \vartheta \begin{bmatrix} \zeta_6 + h_1 \\ \delta_6 + g_1 \end{bmatrix}_{y^6}^{\frac{1}{2}} \bar{\vartheta} \begin{bmatrix} \zeta_6 + h_2 \\ \delta_6 + g_2 \end{bmatrix}_{\bar{w}^6}^{\frac{1}{2}} \bar{\vartheta} \begin{bmatrix} \zeta_6 + h_1 \\ \delta_6 + g_1 \end{bmatrix}_{\bar{y}^6}^{\frac{1}{2}} \\ & \bar{\vartheta} \begin{bmatrix} k \\ l \end{bmatrix}_{\bar{\psi}}^5 \bar{\vartheta} \begin{bmatrix} k + h_2 \\ l + g_2 \end{bmatrix}_{\bar{\eta}^1} \bar{\vartheta} \begin{bmatrix} k + h_1 \\ l + g_1 \end{bmatrix}_{\bar{\eta}^2} \bar{\vartheta} \begin{bmatrix} k - h_1 - h_2 \\ l - g_1 - g_2 \end{bmatrix}_{\bar{\eta}^3} \\ & \bar{\vartheta} \begin{bmatrix} \rho \\ \sigma \end{bmatrix}_{\bar{\phi}^{1,2}}^2 \bar{\vartheta} \begin{bmatrix} \rho + a + k \\ \sigma + b + l \end{bmatrix}_{\bar{\phi}^{3,4}}^2 \bar{\vartheta} \begin{bmatrix} \rho + a + k + H \\ \sigma + b + l + G \end{bmatrix}_{\bar{\phi}^{5,6}}^2 \bar{\vartheta} \begin{bmatrix} \rho + H \\ \sigma + G \end{bmatrix}_{\bar{\phi}^{7,8}}^2 \end{aligned} \quad (5.2)$$

In eq. (5.2), the modular invariant phase ϕ encodes the GGSO phase matrix and the spin statistics are encompassed in the phase $a+b$. The indices a, b are associated with the spacetime fermions ψ^μ , ζ_i relate to the internal 12 internal left and right moving degrees of freedom, h_1 and h_2 correspond to the orbifold twists and k, l, ρ, σ, H, G relate to the 16 additional right moving fermions.

We remark that while in all previous papers the systematic analysis of the partition function and vacuum structure was applied exclusively to S -models, the analysis in our paper is the first in which it is applied to \tilde{S} -based models. That it should work is *a priori* not at all guaranteed. We highlight that the key difference in the \tilde{S} -model is the appearance of indices a, b in the last line of eq. (5.2), indicating the coupling of ψ^μ to the hidden sector fermions within $\tilde{\mathbf{S}}$. The above eq. (5.2) is still only valid at the FFP and so if we allow ourselves to move in the moduli space, we need to rewrite the partition function accordingly.

For the $\mathbb{Z}_2 \times \mathbb{Z}_2$ orbifold, the three internal tori associated with the $\Gamma_{2,2}$ lattice, are parametrised by three complex structure moduli and three Kähler moduli. We can express the partition function in a way that makes the dependence on these geometric moduli, T and U , manifest

$$\begin{aligned}
Z &= \frac{1}{\eta^{12}\bar{\eta}^{24}} \frac{1}{2^3} \sum_{\substack{a,k,\rho \\ b,l,\sigma}} \frac{1}{2^6} \sum_{\substack{\zeta_i \\ \delta_i}} \frac{1}{2^3} \sum_{\substack{h_1, h_2, H \\ g_1, g_2, G}} (-1)^{a+b+\phi} \begin{bmatrix} a & k & \rho & \zeta_i & h_1 & h_2 & H \\ b & l & \sigma & \delta_i & g_1 & g_2 & G \end{bmatrix} \\
&\vartheta \begin{bmatrix} a \\ b \end{bmatrix}_{\psi^\mu} \vartheta \begin{bmatrix} a+h_2 \\ b+g_2 \end{bmatrix}_{\chi^{1,2}} \vartheta \begin{bmatrix} a+h_1 \\ b+g_1 \end{bmatrix}_{\chi^{3,4}} \vartheta \begin{bmatrix} a-h_1-h_2 \\ b-g_1-g_2 \end{bmatrix}_{\chi^{5,6}} \\
&\Gamma_{2,2}^1 \left[\begin{array}{cc|c} H_1 & H_2 & h_2 \\ G_1 & G_2 & g_2 \end{array} \right] (T^{(1)*}, U^{(1)*}) \\
&\Gamma_{2,2}^2 \left[\begin{array}{cc|c} H_3 & H_4 & h_1 \\ G_3 & G_4 & g_1 \end{array} \right] (T^{(2)*}, U^{(2)*}) \\
&\Gamma_{2,2}^3 \left[\begin{array}{cc|c} H_5 & H_6 & h_1+h_2 \\ G_5 & G_6 & g_1+g_2 \end{array} \right] (T^{(3)*}, U^{(3)*}) \\
&\bar{\vartheta} \begin{bmatrix} k \\ l \end{bmatrix}_{\bar{\psi}}^5 \bar{\vartheta} \begin{bmatrix} k+h_2 \\ l+g_2 \end{bmatrix}_{\bar{\eta}^1} \bar{\vartheta} \begin{bmatrix} k+h_1 \\ l+g_1 \end{bmatrix}_{\bar{\eta}^2} \bar{\vartheta} \begin{bmatrix} k-h_1-h_2 \\ l-g_1-g_2 \end{bmatrix}_{\bar{\eta}^3} \\
&\bar{\vartheta} \begin{bmatrix} \rho \\ \sigma \end{bmatrix}_{\bar{\phi}^{1,2}}^2 \bar{\vartheta} \begin{bmatrix} \rho+a+k \\ \sigma+b+l \end{bmatrix}_{\bar{\phi}^{3,4}}^2 \bar{\vartheta} \begin{bmatrix} \rho+a+k+H \\ \sigma+b+l+G \end{bmatrix}_{\bar{\phi}^{5,6}}^2 \bar{\vartheta} \begin{bmatrix} \rho+H \\ \sigma+G \end{bmatrix}_{\bar{\phi}^{7,8}}^2 .
\end{aligned} \tag{5.3}$$

where, at the FFP, $(T, U) = (T_1 + iT_2, U_1 + iU_2) = (T^*, U^*) = (i, \frac{i}{2})$, and we define Γ as:

$$\begin{aligned}
\Gamma_{2,2} \left[\begin{array}{cc|c} H_1 & H_2 & h_2 \\ G_1 & G_2 & g_2 \end{array} \right] (i, \frac{i}{2}) &= \frac{1}{4} \sum_{\zeta_i, \delta_i \in \mathbb{Z}} (-1)^{(\zeta_i+h_2)G_i + (\delta_i+g_2)H_i + H_i G_i} \\
&\vartheta \begin{bmatrix} \zeta_1 \\ \delta_1 \end{bmatrix}_{w^1}^{\frac{1}{2}} \vartheta \begin{bmatrix} \zeta_1+h_2 \\ \delta_1+g_2 \end{bmatrix}_{y^1}^{\frac{1}{2}} \bar{\vartheta} \begin{bmatrix} \zeta_1 \\ \delta_1 \end{bmatrix}_{\bar{w}^1}^{\frac{1}{2}} \bar{\vartheta} \begin{bmatrix} \zeta_1+h_2 \\ \delta_1+g_2 \end{bmatrix}_{\bar{y}^1}^{\frac{1}{2}} \\
&\vartheta \begin{bmatrix} \zeta_2 \\ \delta_2 \end{bmatrix}_{w^2}^{\frac{1}{2}} \vartheta \begin{bmatrix} \zeta_2+h_2 \\ \delta_2+g_2 \end{bmatrix}_{y^2}^{\frac{1}{2}} \bar{\vartheta} \begin{bmatrix} \zeta_2 \\ \delta_2 \end{bmatrix}_{\bar{w}^2}^{\frac{1}{2}} \bar{\vartheta} \begin{bmatrix} \zeta_2+h_2 \\ \delta_2+g_2 \end{bmatrix}_{\bar{y}^2}^{\frac{1}{2}} .
\end{aligned} \tag{5.4}$$

The dependence on the geometric moduli is contained in the untwisted sectors, i.e. the sectors where $h_i = g_i = 0$, so we also define the following:

$$\Gamma_{2,2} \left[\begin{array}{c|c} H_1 & H_2 \\ G_1 & G_2 \end{array} \middle| 0 \right] (T, U) = \sum_{m_i n_i \in \mathbb{Z}} q^{\frac{1}{2}|P_L(T,U)|^2} \bar{q}^{\frac{1}{2}|P_R(T,U)|^2} e^{i\pi(G_1 m_1 + G_2 n_2)} \quad (5.5)$$

where

$$P_L = \frac{1}{\sqrt{2T_2U_2}} \left[m_2 + \frac{H_2}{2} - Um_1 + T(n_1 + \frac{H_1}{2} + Un_2) \right] \quad (5.6)$$

$$P_R = \frac{1}{\sqrt{2T_2U_2}} \left[m_2 + \frac{H_2}{2} - Um_1 + \bar{T}(n_1 + \frac{H_1}{2} + Un_2) \right] \quad (5.7)$$

which is equal to the previous expression at the FFP $(T, U) = (T^*, U^*)$. Eqs. (5.5), (5.6) and (5.7) are independent of a, b and so are identical in S - and \tilde{S} -models. From this the q -expansion can be found and analysed, using standard definitions of ϑ and η functions that can be found in Appendix A of [21], for example. The general form of the q -expansion can be expressed as

$$Z = \sum_{m,n} a_{m,n} q^m \bar{q}^n. \quad (5.8)$$

5.2 Potential

The resulting one-loop potential determines the stability of the model, with the ideal being a consistent theory sitting in a global minima of the potential. Having determined a method of finding the partition function at general locations in the moduli space, we can observe how the one loop potential varies over the moduli space by integrating the partition function over the fundamental domain of the torus amplitude:

$$\begin{aligned} V_{1-loop} &= -\frac{1}{2} \frac{\mathcal{M}^4}{(2\pi)^4} \int_{\mathcal{F}} \frac{d^2\tau}{\tau_3^2} Z(\tau, \bar{\tau}; T^{(i)}, U^{(i)}) \\ &= -\frac{1}{2} \frac{\mathcal{M}^4}{(2\pi)^4} \int_{\mathcal{F}} \frac{d^2\tau}{\tau_3^2} \sum a_{m,n} q^m \bar{q}^n \\ &= -\frac{1}{2} \frac{\mathcal{M}^4}{(2\pi)^4} \sum a_{m,n} I_{m,n} \end{aligned} \quad (5.9)$$

where $\frac{d^2\tau}{\tau_3^2}$ is the modular invariant measure and the fundamental domain, \mathcal{F} , is defined as

$$\mathcal{F} = \{ \tau \in \mathbb{C} \mid |\tau|^2 > 1 \quad \wedge \quad |\tau_1| < 0.5 \}. \quad (5.10)$$

This corresponds to the spacetime cosmological constant of the theory, with the factor $-\frac{1}{2} \frac{\mathcal{M}^4}{(2\pi)^4}$ relating the worldsheet potential to the spacetime potential. For example, supersymmetric models with $a_{ij} = 0$ have a vanishing cosmological constant.

Whilst all of the models that fulfil the phenomenological criteria are found to have finite potential, only a fraction are stable at the FFP, as there is no inherent reason for the minima to be located here. This feature is a result of \mathbf{e}_i basis vectors which generally break T -duality. In contrast, models that use \mathbf{T}_i basis vectors [10] appear to always sit in minima at the FFP. Moving away from the FFP typically leads to divergences.

These divergences arise from level-matched and non-level matched tachyons, which can be understood through the modular integral results

$$I_{m,n} = \begin{cases} \infty & \text{if } m+n < 0 \text{ and } m-n \notin \mathbb{Z} \setminus \{0\} \\ \text{Finite} & \text{otherwise.} \end{cases} \quad (5.11)$$

With T and U being complex moduli, we have 6 complex internal degrees of freedom. It is impractical to vary all 6 and determine the shape of the potential. Following the logic used in refs. [10, 11, 25], we choose to vary: $\text{Im}(T^{(1)}) = T_2$ associated with the volume of the first torus and $\text{Im}(U^{(1)}) = U_2$, the imaginary component of $U^{(1)}$, associated with the shape, while leaving the moduli of the second and third tori fixed at the free fermionic point. The modulus T_2 has previously been studied in relation to explicit and Scherk-Schwarz spontaneous supersymmetry breaking [11], where, in the latter case, SUSY can be restored as $T_2 \rightarrow \infty$. We have chosen here to vary the same moduli for consistency and comparison between S -models and our \tilde{S} -models.

6 Classification Results

Now that we have defined our classification constraints we can classify models within the full space of $2^{66} \sim 7.4 \times 10^{19}$ GGSO phase configurations. Due to constraints on computational power and time, we take a sample size of 10^9 models, which demonstrates the statistics well. The results of this search are given in Table 5. Of the sampled models, only 0.531% were free from level-matched tachyons and we recall that this constraint necessitates that observable enhancements are absent. We then choose to project hidden enhancements leaving 0.487% of the sample. Of the remaining models, 0.00308% of the sample satisfy the constraint on the net chirality of spinorial $\mathbf{16}/\overline{\mathbf{16}}$'s of eq. (4.13). This further reduces to 0.00307% when accommodating for the required vectorial $\mathbf{10}$ of eq. (4.22). Finally, we see that 84 models in our sample obey the TQMC conditions and so we do produce viable, fertile models at a frequency of 8.40×10^{-8} . Although the condition $a_{00} = N_b - N_f = 0$ is not a phenomenological requirement, we show that in our sample 4 models were found that obey this at the FFP.

Constraint	Quantity	Probability
No Constraints	1.00×10^9	1
Tachyon Free	5,309,285	5.309×10^{-3}
No Observable Enhancements	5,309,285	5.309×10^{-3}
No Hidden Enhancements	4,865,203	4.865×10^{-3}
$N_{\mathbf{16}} - N_{\overline{\mathbf{16}}} \geq 6$	30,773	3.077×10^{-5}
$N_{\mathbf{10}} \geq 1$	30,717	3.072×10^{-5}
TQMC	84	8.40×10^{-8}
$a_{00} = N_b^{(0)} - N_f^{(0)} = 0$	4	4.00×10^{-9}

Table 5: Frequency of models after each additional constraint is applied to the sample of 1.00×10^9

Further analysis of these models shows that they all have finite potential at the FFP, confirming the absence of level matched tachyons. As there are no complex boundary conditions in our models, non-level matched tachyons that would cause divergences are

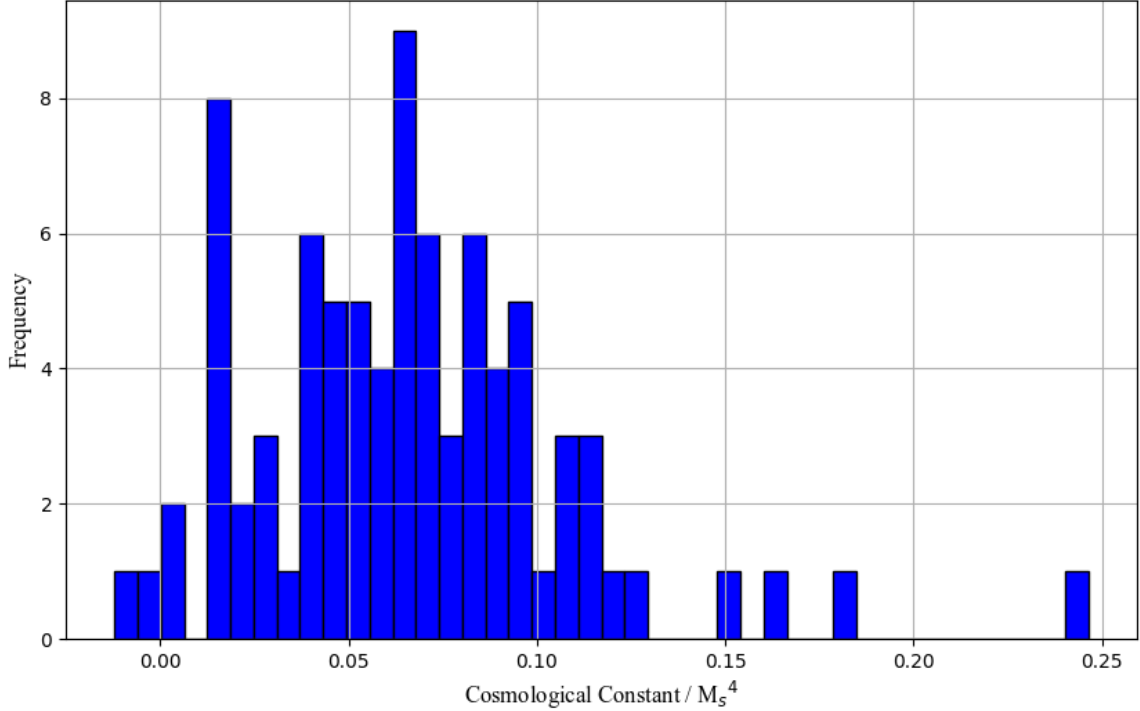


Figure 1: Histogram to show the distribution of the Cosmological Constant of the 84 fertile cores at the Free Fermionic Point.

absent from the spectrum at the FFP. However the FFP is not necessarily the minimum in potential. This is demonstrated in the next section.

We mostly find models with positive values of the potential at the one loop level in this sample, representing De Sitter vacua. The distribution of the Cosmological Constants at the FFP is given in 1. Only 2 of the 84 fertile cores have negative cosmological constant at the FFP, and these 2 very quickly become divergent away from this point. \tilde{S} -models are more inclined to positive values of the potential. A significant factor in this is the projection of massive bosonic superpartners to higher masses, reducing their contribution to the potential.

7 Example Model

Here we present an example of a model that meets all of the criteria in Table 5, save for $a_{00} = 0$. Below is the GGSO matrix of the model, from which we can derive the partition function.

$$C \begin{bmatrix} v_i \\ v_j \end{bmatrix} = \begin{matrix} \mathbb{1} & \tilde{\mathbf{S}} & \mathbf{e}_1 & \mathbf{e}_2 & \mathbf{e}_3 & \mathbf{e}_4 & \mathbf{e}_5 & \mathbf{e}_6 & \mathbf{b}_1 & \mathbf{b}_2 & \mathbf{z}_1 & \mathbf{z}_2 \\ \tilde{\mathbf{S}} & \begin{pmatrix} -1 & 1 & 1 & -1 & 1 & 1 & -1 & 1 & 1 & 1 & 1 & 1 \\ 1 & -1 & -1 & 1 & 1 & 1 & -1 & -1 & 1 & 1 & -1 & 1 \\ 1 & -1 & -1 & -1 & 1 & 1 & -1 & 1 & -1 & 1 & 1 & 1 \\ -1 & 1 & -1 & 1 & -1 & -1 & 1 & -1 & -1 & 1 & -1 & -1 \\ 1 & 1 & 1 & -1 & -1 & 1 & 1 & 1 & 1 & -1 & -1 & 1 \\ 1 & 1 & 1 & -1 & 1 & -1 & 1 & 1 & 1 & -1 & -1 & 1 \\ -1 & -1 & -1 & 1 & 1 & 1 & 1 & 1 & -1 & -1 & 1 & -1 \\ 1 & -1 & 1 & -1 & 1 & 1 & 1 & -1 & 1 & -1 & 1 & -1 \\ 1 & -1 & -1 & -1 & 1 & 1 & -1 & 1 & 1 & -1 & -1 & -1 \\ \mathbf{b}_1 & 1 & -1 & -1 & -1 & 1 & 1 & -1 & 1 & 1 & -1 & -1 \\ \mathbf{b}_2 & 1 & -1 & 1 & 1 & -1 & -1 & -1 & -1 & -1 & 1 & -1 \\ \mathbf{z}_1 & 1 & 1 & 1 & -1 & -1 & -1 & 1 & 1 & -1 & -1 & 1 \\ \mathbf{z}_2 & 1 & -1 & 1 & -1 & 1 & 1 & -1 & -1 & -1 & -1 & 1 \end{pmatrix} & & & & & & & & & & & & \end{matrix} \quad (7.1)$$

Crucially, it is important to convert our basis vectors in the FFF to the following S -matrix, from which we can calculate the partition function in the form discussed in Section 5.1. We adopt the formalism developed in ref. [11, 33, 30] to convert from the FFF basis set phases to the index set used in the expression for the partition function in eq. (5.2)

$$S = \begin{matrix} & a & k & \rho & H_1 & H_2 & H_3 & H_4 & H_5 & H_6 & h_1 & h_2 & H \\ \mathbb{1} & \begin{pmatrix} 1 & 1 & 1 & 1 & 1 & 1 & 1 & 1 & 1 & 1 & 0 & 0 & 0 \\ 1 & 0 & 0 & 0 & 0 & 0 & 0 & 0 & 0 & 0 & 0 & 0 & 0 \\ 0 & 0 & 0 & 1 & 0 & 0 & 0 & 0 & 0 & 0 & 0 & 0 & 0 \\ 0 & 0 & 0 & 0 & 1 & 0 & 0 & 0 & 0 & 0 & 0 & 0 & 0 \\ 0 & 0 & 0 & 0 & 0 & 1 & 0 & 0 & 0 & 0 & 0 & 0 & 0 \\ 0 & 0 & 0 & 0 & 0 & 0 & 0 & 1 & 0 & 0 & 0 & 0 & 0 \\ 0 & 0 & 0 & 0 & 0 & 0 & 0 & 0 & 1 & 0 & 0 & 0 & 0 \\ 1 & 1 & 0 & 0 & 0 & 0 & 0 & 0 & 0 & 0 & 1 & 0 & 0 \\ 1 & 1 & 0 & 0 & 0 & 0 & 0 & 0 & 0 & 0 & 0 & 1 & 0 \\ 0 & 0 & 1 & 0 & 0 & 0 & 0 & 0 & 0 & 0 & 0 & 0 & 1 \\ 0 & 0 & 0 & 0 & 0 & 0 & 0 & 0 & 0 & 0 & 0 & 0 & 1 \end{pmatrix} & & & & & & & & & & & & \end{matrix} \quad (7.2)$$

The partition function for this model at the FFP, calculated to order $\mathcal{O}(2)$, is:

$$\begin{aligned} Z = & -200 + \frac{2}{\bar{q}} + 74560\bar{q} + \frac{448\bar{q}^{\frac{1}{2}}}{q^{\frac{1}{2}}} + \frac{608\bar{q}^{\frac{5}{8}}}{q^{\frac{3}{8}}} + \frac{6912\bar{q}^{\frac{3}{4}}}{q^{\frac{1}{4}}} + \frac{33280\bar{q}^{\frac{7}{8}}}{q^{\frac{1}{8}}} - 384\bar{q}^{\frac{1}{8}}q^{\frac{1}{8}} \\ & - 2832\bar{q}^{\frac{1}{4}}q^{\frac{1}{4}} - 9488\bar{q}^{\frac{3}{8}}q^{\frac{3}{8}} + \frac{184q^{\frac{1}{2}}}{\bar{q}^{\frac{1}{2}}} - 16000\bar{q}^{\frac{1}{2}}q^{\frac{1}{2}} + \frac{432q^{\frac{5}{8}}}{\bar{q}^{\frac{3}{8}}} - 16368\bar{q}^{\frac{5}{8}}q^{\frac{5}{8}} \\ & + \frac{960q^{\frac{3}{4}}}{\bar{q}^{\frac{1}{4}}} + 131200\bar{q}^{\frac{3}{4}}q^{\frac{3}{4}} + \frac{832q^{\frac{7}{8}}}{\bar{q}^{\frac{1}{8}}} + 600768\bar{q}^{\frac{7}{8}}q^{\frac{7}{8}} - 3264q \\ & + \frac{32q}{\bar{q}} + 1369472\bar{q}q + \frac{8q^{\frac{1}{4}}}{p^{\frac{3}{4}}} + \frac{16q^{\frac{3}{8}}}{p^{\frac{5}{8}}}. \end{aligned} \quad (7.3)$$

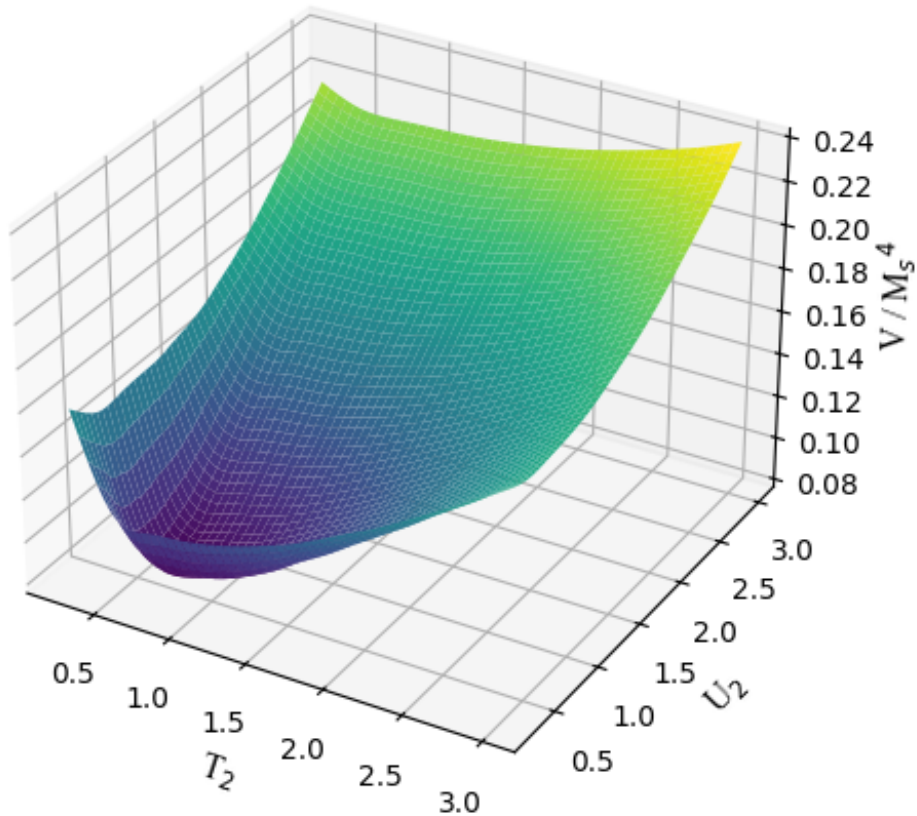


Figure 2: Graph to show an example of a stable \tilde{S} -Model, with a minimum in the potential, V , away from the FFP. The minimum in potential is located at $(\frac{3}{4}, \frac{3}{4})$, with $V_{\min} = \Lambda_{\min} = 0.08276\mathcal{M}^4$

Integrating the partition function we find the model to have finite potential, Λ , at the FFP

$$\Lambda = 0.08707\mathcal{M}^4. \quad (7.4)$$

The graphs are produced by spanning T_2 and U_2 in the region $\frac{1}{4} \leq T_2, U_2 \leq 3$, and interpolating between these points. To this accuracy we find the minimum in potential sits at $(\frac{3}{4}, \frac{3}{4})$, not at the FFP

$$\Lambda_{\min} = 0.08276\mathcal{M}^4. \quad (7.5)$$

Comparing these graphs to S -models in [11], we can see that a feature they share is that the potential diverges as T_2 increase. In these models this is a result of the breaking of supersymmetry explicitly, not spontaneously. In this case the potentials of \tilde{S} - and S -models share a similar distribution and become indistinguishable as $T_2 \rightarrow \infty$.

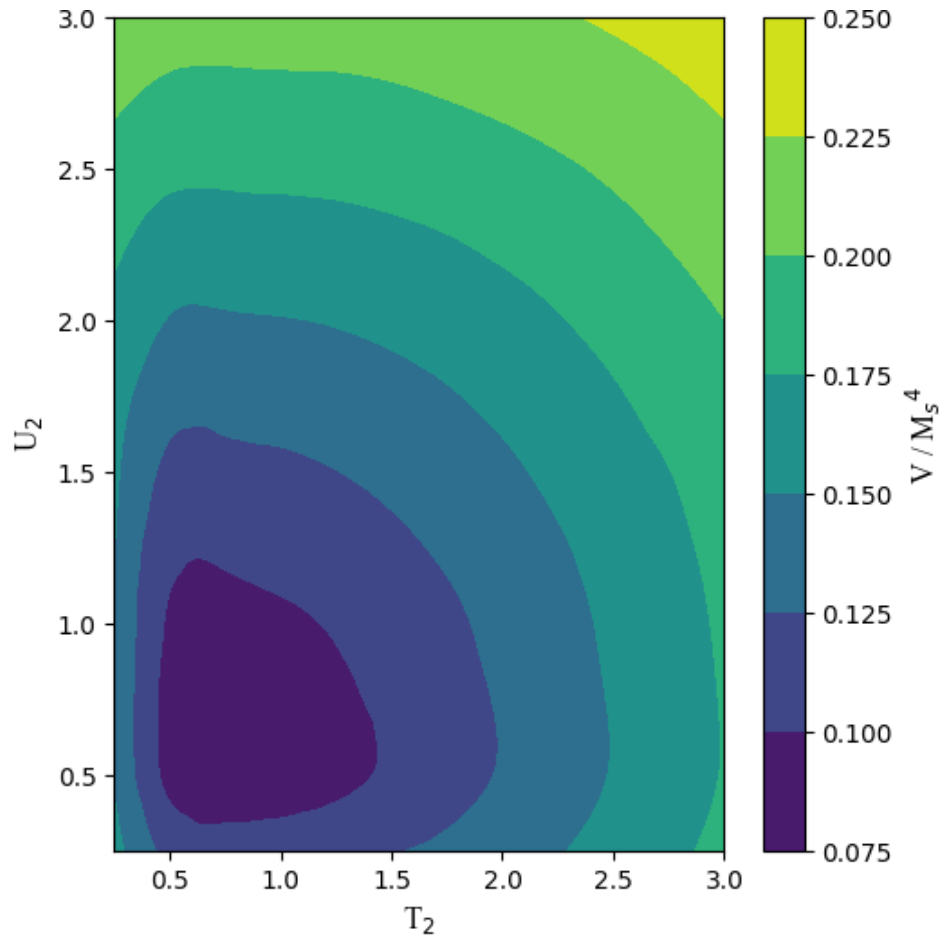


Figure 3: Contour plot of Figure 2

8 Discussion and Conclusion

In this paper we analysed the space of heterotic-string \tilde{S} -models in the Free Fermionic Formalism. These models are non-supersymmetric $SO(10)$ string models and so lose some of the appealing features of supersymmetric models. In general the spectrum will contain tachyonic states and thus be unstable at the FFP. Computer programs, written in C++, were developed and utilised to classify a random sample of 1.0×10^9 \tilde{S} -vacua against phenomenological conditions, in search of models compatible with SM data, and with similar features to previously studied S -models. Following a similar procedure to previous analysis [22, 21, 10], these conditions are chosen to be: projection of all level-matched tachyons; accommodating 3 spinorial generations of SM particles; production of 1 vectorial state compatible with the Higgs doublet; TQMC survival; and having a finite, stable potential around the FFP. We also look for models that mimic supersymmetry with equal numbers of massless bosons and fermions. In Section 6 these results are outlined. Of the 10^9 GGSO matrices which were sampled, only 0.5309% were tachyon free. Of these, only 0.003072% were compatible with the SM fermion generations and Higgs particle. $(8.4 \times 10^{-5})\%$ of our sample adhered to the TQMC conditions, with 4 out of 10^9 showing Bose-Fermi degeneracy at the massless level.

Crucially, in Section 7, we adapted the notation and methodology of [11, 12] and applied it to non-supersymmetric \tilde{S} -models. We demonstrated that the \tilde{S} -models provide an abundance of non-supersymmetric vacua, which are both compatible with fertility conditions, and have finite one-loop potential at the FFP. Our sample suggests that 98% of these vacua have positive Cosmological Constant, corresponding to a De Sitter space. This statistic is only based on a sample of 84 models and so is likely to be inaccurate, however it does demonstrate that both positive and negative cosmological constants can be found. Fertile models can be constructed that sit at the minima of the potential at or around the FFP, when the geometric moduli $T_2^{(1)}$ and $U_2^{(1)}$ are varied. It is important to note that since the other geometric moduli were fixed at the FFP, we do not know the behaviour of the models when $T_1^{(1)}$ and $U_1^{(1)}$ are varied. Similarly, we can not speak to the behaviour of the model for values of $T^{(2,3)}$ and $U^{(2,3)}$ away from the FFP.

In regard to the example model in Section 7 for which the minimum in potential sits away from the FFP, we cannot guarantee that the fertility conditions are satisfied at this point. We also can't say whether this is the global minimum across all moduli space. We can only conclude that the model remain tachyon free in the moduli space we have sampled, but further analysis of the spectrum away from the FFP would need to be undertaken. Furthermore, we only calculate the potential at the one loop level. Another factor in the stability of the model and value of the potential is the existence of tadpole diagrams and uplifts [11, 12]. A thorough exploration of these effects on the model would be required before drawing further conclusions on stability of models, and their compatibility with cosmological data such as the cosmological constant. In this regard, this work simplifies the picture, but demonstrates that these models warrant further investigation.

A limiting factor to be addressed in this work is computational time. Randomly sampling such a large space is not the most efficient way to find fertile cores [35], but was necessary in this work to find a representative statistical sample. In exploring such a large space of vacua, we define the fertility conditions necessary to find consistent string vacua. This can act as a jumping off point should these models be analysed further, mitigating

a portion of the computing time and producing an increased frequency of fertile models. For example, further work to break these models down to Pati-Salam [22] or Standard-like Models could be done to analyse the effect this has on the potential.

However, calculating the partition functions of the fertile models away from the FFP was the most inefficient aspect of this work. This is due to the large dimensionality and complexity of the calculation. Because of this, we are limited to only exploring the effect of $T_2^{(1)}$ and $U_2^{(1)}$ on the potential. An appealing solution would be to employ more advanced computational techniques such as machine learning, which are better suited for handling high-dimensional computation and categorisation problems, and are likely to increase efficiency. This should allow us to explore a greater proportion of the moduli space and perhaps lead to a greater understanding of the potential.

As there is no way to restore supersymmetry in \tilde{S} -models, it would seem the viability of these models relies on the absence of supersymmetry from Nature all the way up to the $SO(10)$ GUT level, and, whilst there is no evidence of supersymmetry at the time of writing, improvements to experiments at CERN and other proposed experiments [47, 48, 49] promise to probe higher energy levels. Should evidence of supersymmetry be discovered, this would raise questions on the relevance of non-supersymmetric \tilde{S} -models to low scale physics. Nevertheless, we comment that exploration of the role of the tachyonic ten dimensional string vacua aims at developing an understanding of the string scale, rather than their potential relevance to low scale physics. It should be viewed more in the context of the underlying theory that unifies the ten dimensional string vacua, or as it is traditionally dubbed as M -theory. It seems plausible that within that context, the tachyonic ten dimensional vacua may play a role.

Acknowledgements

This research was supported in part by grant NSF PHY-2309135 to the Kavli Institute for Theoretical Physics (KITP). The work of LD is supported by STFC and LIV.INNO. The work of ARDA is supported in part by EPSRC grant EP/T517975/1. AEF would like to thank the Kavli Institute for Theoretical Physics and the CERN theory division for hospitality.

References

- [1] A. E. Faraggi, D. V. Nanopoulos, and K. Yuan. “A standard-like model in the four-dimensional free fermionic string formulation”. In: *Nuclear Physics* 335 (1990), pp. 347–362.
- [2] A. E. Faraggi. “A new standard-like model in the four dimensional free fermionic string formulation”. In: *Physics Letters B* 278.1-2 (1992), pp. 131–139.
- [3] G. Cleaver, A. Faraggi, and D. V. Nanopoulos. “String derived MSSM and M-theory unification”. In: *Physics Letters B* 455.1-4 (1999), pp. 135–146.
- [4] J. M. Ashfaque, P. Athanasopoulos, A. E. Faraggi, and H. Sonmez. “Non-tachyonic semi-realistic non-supersymmetric heterotic-string vacua”. In: *The European Physical Journal C* 76 (2015), pp. 1–17.
- [5] S. Abel, K. R. Dienes, and E. Mavroudi. “Towards a nonsupersymmetric string phenomenology”. In: *Physical Review D* 91 (2015), p. 126014.
- [6] M. Blaszczyk, S. G. Nibbelink, O. Loukas, and F. Ruehle. “Calabi-Yau compactifications of non-supersymmetric heterotic string theory”. In: *Journal of High Energy Physics* 2015 (2015), pp. 1–43.
- [7] H. Itoyama and S. Nakajima. “Stability, enhanced gauge symmetry and suppressed cosmological constant in 9D heterotic interpolating models”. In: *Nuclear Physics* 958 (2020), p. 115111.
- [8] P. Boyle Smith, Y.-H. Lin, Y. Tachikawa, and Y. Zheng. “Classification of chiral fermionic CFTs of central charge ≤ 16 ”. In: *SciPost Physics* 16.2 (2024), p. 058.
- [9] M. Blaszczyk, S. G. Nibbelink, O. Loukas, and S. Ramos-Sanchez. “Non-supersymmetric heterotic model building”. In: *Journal of High Energy Physics* 2014.10 (2014), pp. 1–33.
- [10] I. Florakis and J. Rizos. “Chiral heterotic strings with positive cosmological constant”. In: *Nuclear Physics B* 913 (2016), pp. 495–533.
- [11] A. R. Avalos Diaz, A. E. Faraggi, V. G. Matyas, and B. Percival. “D-term uplifts in nonsupersymmetric heterotic string models”. In: *Physical Review D* 108.8 (2023), p. 086007.
- [12] A. R. D. Avalos, A. E. Faraggi, V. G. Matyas, and B. Percival. “Fayet–Iliopoulos D-term in non-supersymmetric heterotic string orbifolds”. In: *The European Physical Journal C* 83.10 (2023), p. 926.
- [13] C. Angelantonj, I. Florakis, G. Leone, and D. Perugini. “Non-supersymmetric non-tachyonic heterotic vacua with reduced rank in various dimensions”. In: *arXiv preprint arXiv:2407.09597* (2024).
- [14] H. Kawai, D. C. Lewellen, and S. H. H. Tye. “Classification of closed-fermionic-string models.” In: *Physical Review D* 34 (1986), pp. 3794–3804.
- [15] L. J. Dixon and J. A. Harvey. “String theories in ten dimensions without spacetime supersymmetry”. In: *Nuclear Physics B* 274.1 (1986), pp. 93–105.
- [16] L. Alvarez-Gaume, P. Ginsparg, G. Moore, and C. Vafa. “An $O(16) \times O(16)$ heterotic string”. In: *Physics Letters B* 171.2-3 (1986), pp. 155–162.

- [17] P. H. Ginsparg and C. Vafa. “Toroidal Compactification of Nonsupersymmetric Heterotic Strings”. In: *Nucl. Phys. B* 289 (1987), p. 414. DOI: 10.1016/0550-3213(87)90387-7.
- [18] H. Itoyama and T. R. Taylor. “Supersymmetry Restoration in the Compactified $O(16) \times O(16)$ -prime Heterotic String Theory”. In: *Phys. Lett. B* 186 (1987), pp. 129–133. DOI: 10.1016/0370-2693(87)90267-X.
- [19] A. Faraggi. “String phenomenology from a worldsheet perspective”. In: *The European Physical Journal C* 79 (Aug. 2019). DOI: 10.1140/epjc/s10052-019-7222-5.
- [20] A. Faraggi, V. Matyas, and B. Percival. “Stable three generation standard-like model from a tachyonic ten dimensional heterotic-string vacuum”. In: *The European Physical Journal C* 80 (Apr. 2020). DOI: 10.1140/epjc/s10052-020-7894-x.
- [21] A. E. Faraggi, V. G. Matyas, and B. Percival. “Towards the classification of tachyon-free models from tachyonic ten-dimensional heterotic string vacua”. In: *Nuclear Physics B* 961 (2020), p. 115231.
- [22] A. E. Faraggi, V. G. Matyas, and B. Percival. “Classification of nonsupersymmetric Pati-Salam heterotic string models”. In: *Physical Review D* 104.4 (2021), p. 046002.
- [23] A. Faraggi, B. Percival, S. Schewe, and D. Wojtczak. “Satisfiability modulo theories and chiral heterotic string vacua with positive cosmological constant”. In: *Physics Letters B* 816 (Mar. 2021), p. 136187. DOI: 10.1016/j.physletb.2021.136187.
- [24] H. Itoyama and S. Nakajima. “Marginal deformations of heterotic interpolating models and exponential suppression of the cosmological constant”. In: *Physics Letters B* 816 (2021), p. 136195. DOI: <https://doi.org/10.1016/j.physletb.2021.136195>.
- [25] I. Florakis, J. Rizos, and K. Violaris-Gountonis. “Super no-scale models with Pati-Salam gauge group”. In: *Nuclear Physics B* 976 (2022), p. 115689.
- [26] Z. K. Baykara, H.-C. Tarazi, and C. Vafa. “New Non-Supersymmetric Tachyon-Free Strings”. In: *arXiv preprint arXiv:2406.00185* (2024).
- [27] Z. K. Baykara, H.-C. Tarazi, and C. Vafa. “The Quasicrystalline String Landscape”. In: *arXiv preprint arXiv:2406.00129* (2024).
- [28] I. Antoniadis and C. Bachas. “4d fermionic superstrings with arbitrary twists”. In: *Nuclear Physics B* 298.3 (1988), pp. 586–612.
- [29] H. Kawai, D. C. Lewellen, and S.-H. H. Tye. “Construction of fermionic string models in four dimensions”. In: *Nuclear Physics B* 288 (1987), pp. 1–76.
- [30] I. Florakis and J. Rizos. “From free-fermionic constructions to orbifolds and back”. In: *JHEP* 01 (2024), p. 151. DOI: 10.1007/JHEP01(2024)151. arXiv: 2310.10438 [hep-th].
- [31] A. E. Faraggi, C. Kounnas, and J. Rizos. “Spinor-Vector Duality in fermionic $Z_2 \times Z_2$ heterotic orbifold models”. In: *Nuclear Physics B* 774.1-3 (2007), pp. 208–231.
- [32] A. Faraggi, C. Kounnas, S. Nooij, and J. Rizos. “Classification of the chiral $Z_2 \times Z_2$ fermionic models in the heterotic superstring”. In: *Nuclear Physics B* 695.1-2 (2004), pp. 41–72.

- [33] V. G. Matyas. “Non-supersymmetric heterotic orbifolds”. PhD thesis. The University of Liverpool (United Kingdom), 2023.
- [34] P. Breitenlohner and D. Z. Freedman. “Positive energy in anti-de Sitter backgrounds and gauged extended supergravity”. In: *Physics Letters B* 115.3 (1982), pp. 197–201.
- [35] A. E. Faraggi, B. Percival, S. Schewe, and D. Wojtczak. “Satisfiability modulo theories and chiral heterotic string vacua with positive cosmological constant”. In: *Physics Letters B* 816 (2021), p. 136187.
- [36] J. C. Pati and A. Salam. “Lepton number as the fourth "color"”. In: *Physical Review D* 10.1 (1974), p. 275.
- [37] I. Antoniadis, G. Leontaris, and J. Rizos. “A three-generation $SU(4) \times O(4)$ string model”. In: *Physics Letters B* 245.2 (1990), pp. 161–168.
- [38] B. Assel, K. Christodoulides, A. E. Faraggi, C. Kounnas, and J. Rizos. “Classification of heterotic Pati–Salam models”. In: *Nuclear Physics B* 844.3 (2011), pp. 365–396.
- [39] A. E. Faraggi, J. Rizos, and H. Sonmez. “Classification of standard-like heterotic-string vacua”. In: *Nuclear Physics B* 927 (2018), pp. 1–34.
- [40] A. E. Faraggi. “Doublet–triplet splitting in realistic heterotic string derived models”. In: *Physics Letters B* 520.3-4 (2001), pp. 337–344.
- [41] A. E. Faraggi. “Yukawa couplings in superstring derived standard like models”. In: *Phys. Rev. D* 47 (1993), pp. 5021–5028. DOI: 10.1103/PhysRevD.47.5021.
- [42] J. Rizos. “Top-quark mass coupling and classification of weakly coupled heterotic superstring vacua”. In: *The European Physical Journal C* 74.6 (2014), p. 2905.
- [43] I. Florakis. “Gravitational threshold corrections in non-supersymmetric heterotic strings”. In: *Nuclear Physics B* 916 (2017), pp. 484–509.
- [44] C. Kounnas and H. Partouche. “Super no-scale models in string theory”. In: *Nucl. Phys. B* 913 (2016), pp. 593–626. DOI: 10.1016/j.nuclphysb.2016.10.001. arXiv: 1607.01767 [hep-th].
- [45] K. R. Dienes. “New string partition functions with vanishing cosmological constant”. In: *Phys. Rev. Lett.* 65 (1990), pp. 1979–1982. DOI: 10.1103/PhysRevLett.65.1979.
- [46] I. Florakis and J. Rizos. “Free Fermionic Constructions of Heterotic Strings”. In: *Handbook of Quantum Gravity*. Springer, 2023, pp. 1–47.
- [47] A. E. Faraggi, M. Guzzi, and A. McEntaggart. “String Derived Z' Model at an Upgraded Superconducting Super Collider”. In: *Letters in High Energy Physics* 2023 (2023).
- [48] M. Narain, L. Reina, A. Tricoli, M. Begel, A. Belloni, T. Bose, A. Boveia, S. Dawson, C. Doglioni, A. Freitas, et al. “The Future of US Particle Physics—The Snowmass 2021 Energy Frontier Report”. In: *arXiv preprint arXiv:2211.11084* (2022).
- [49] E. S. G. Collaboration et al. “Update of the European Strategy for Particle Physics”. In: *CERN Council, Geneva* 10 (2020), p. 88.